Electronic Supplementary Information (ESI)

Superparamagnetic Nalidixic acid grafted Magnetite (Fe_3O_4/NA) for Rapid and Efficient Mercury Removal from Water

Syed M. Husnain[a], Jae-Hawn Kim [a], Chung-Seop Lee [a], Yoon-Young Chang [b], Wooyong Um [c,d], Yoon-Seok Chang [a*]

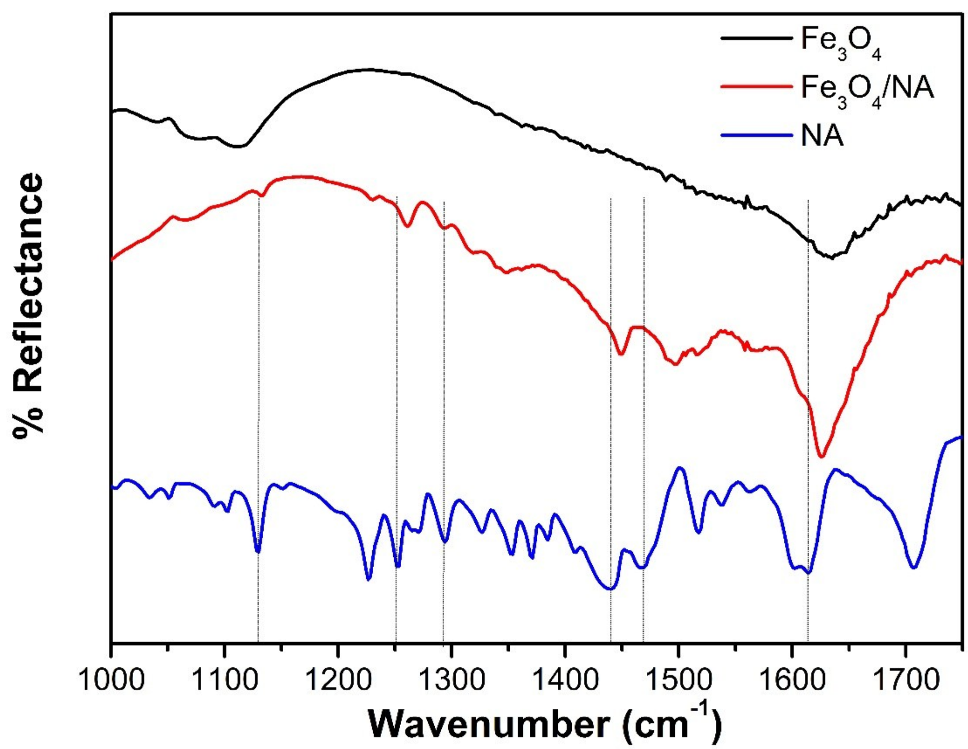

Fig. S1 FTIR of Fe_3O_4, Fe_3O_4/NA and NA

The FTIR spectra of pure NA were plotted in the wavenumbers ranging from 1000 to 1750 cm^{-1} along with Fe_3O_4 and Fe_3O_4/NA as illustrated in Fig. S1. Strong bands centered at 1440 and 1467 cm^{-1} corresponds to symmetrical stretching of C=C and C=N vibrations in pure NA, these two vibrations bands shifted to 1450 and 1490 cm^{-1}, respectively after the NA grafting onto Fe_3O_4. The band located at 1630 cm^{-1} in Fe_3O_4/NA might be ascribed to dual interaction of C=C asymmetric ring stretching vibrations at 1617 cm^{-1} and/or C=O carboxylic acid stretching at 1700 cm^{-1} of NA. Minor shift to higher wavenumbers was also noticed after grafting of NA onto Fe_3O_4 for the bands ascribed to C-H deformation (at 1130 and 1253 cm^{-1}) and COH deformation at 1295 cm^{-1}. All aforementioned observations confirm the existence of strong chemical interactions of NA with Fe_3O_4 surface.

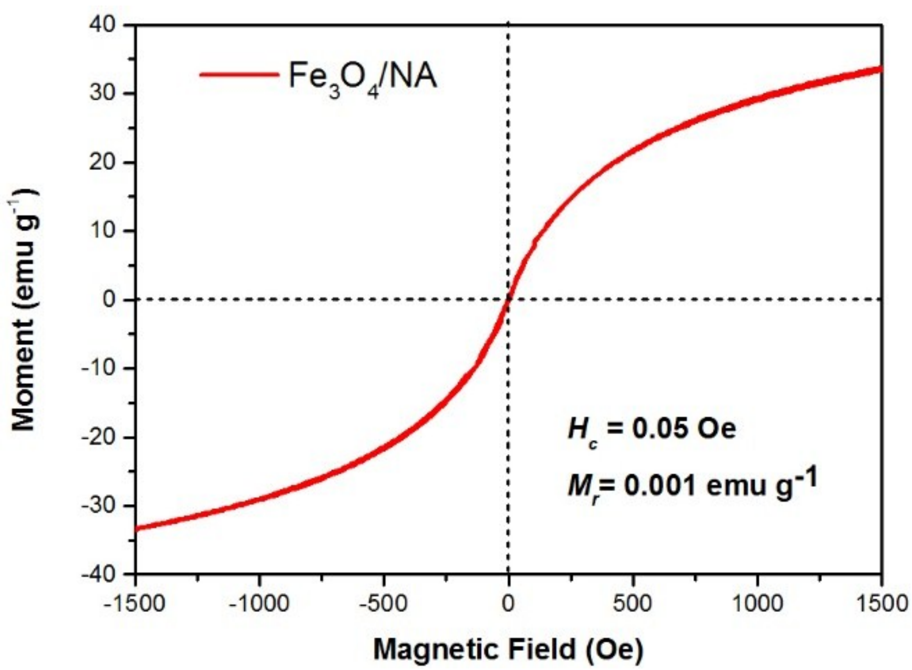

Fig. S2 Magnified hysteresis loop of Fe_3O_4/NA

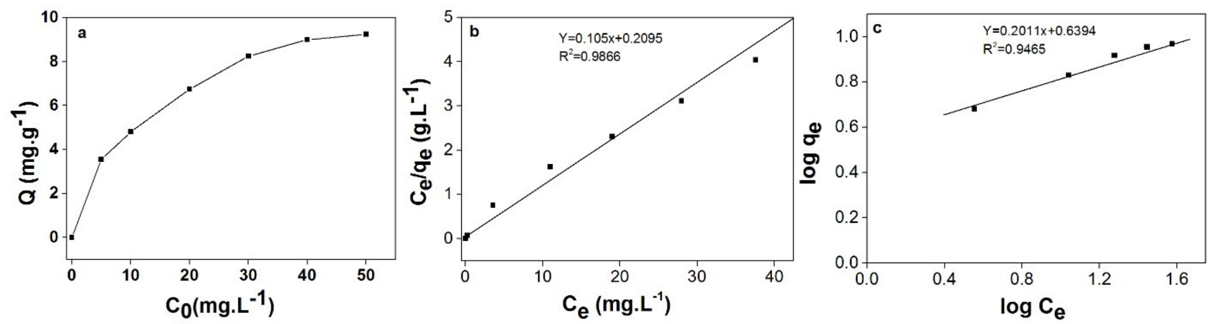

Fig. S3 (a) Relationship between the initial concentration of Hg(II) and the equilibrium adsorption (*Q*). Langmuir (b) and Freundlich (c) isotherm of adsorption of Hg(II) onto the Fe_3O_4/NA

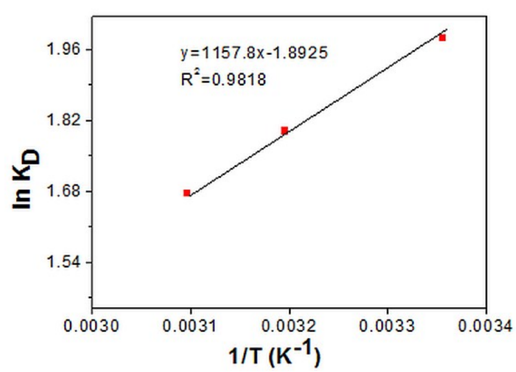

Fig. S4 Thermodynamic study of adsorption of mercury onto Fe_3O_4/NA

Table S1 Kinetic parameters for Hg(II) adsorption on bare Fe_3O_4 andFe_3O_4/NA

	Bare Fe_3O_4	**Fe_3O_4/NA**
Pseudo-first-order model		
$\boldsymbol{k_1}$ **(min^{-1})**	0.04	0.09
$\boldsymbol{q_{e,exp}}$ **(mg g^{-1})**	0.31	0.80
$\boldsymbol{q_{e,cal}}$ **(mg g^{-1})**	2.13	3.60
R^2	0.92	0.97
Pseudo-second-order model		
$\boldsymbol{k_2}$ **(g mg^{-1} min^{-1})**	0.6	0.35
$\boldsymbol{q_{e,exp}}$ **(mg g^{-1})**	2.14	3.63
$\boldsymbol{q_{e,cal}}$ **(mg g^{-1})**	2.13	3.60
R^2	0.99	0.99

Table S2 Comparison of adsorption capacity of mercury for different adsorbents

Adsorbent	Capacity	Temperature	pH	Time	Reference
Clay	0.23 mg g^{-1}	293 K	5.5	12-14 h	[50]
Fly ash	2.50 mg g^{-1}	303 K	3.5-4.5	3 h	[51]
Rice husk ash	6.72 mg g^{-1}	303 K	5.6-5.8	30 min	[52]
Activated Carbon	5.20 mg g^{-1}	283 K	n.a	500 min	[53]
Magnetic NPs modified with 2-mercaptobenzothiazole	0.59 mg g^{-1}	298 K	9	4 min	[54]
Thiol-modified magnetite beads-porous materials	14 mg g^{-1}	n.a	2	1 h	[55]
Silica-graft dimethyl amino ethyl methacrylate	8.10 mg g^{-1}	n.a	4	24 h	[56]
Naphthalimide-functionalized magnetic nanosensor	5.6 mg g^{-1}	298 K	n.a	Overnight ~12 h	[57]
Dithiocarbamate grafted on magnetite particles	142-206 mg g^{-1}	295 K	7	96 h	[58]
Nalidixic acid grafted Magnetic nanoparticles	9.52 mg g^{-1}	298 K	6	1 h	This Study

Table S3 Thermodynamic parameters for adsorption of Hg(II) at different temperature

Temperature (K)	ΔG^o (kJ mol^{-1})	ΔH° (kJ mol^{-1})	ΔS^o (J mol^{-1} K^{-1})
298	-4.91	-9.63	-15.73
313	-4.76		
323	-4.50		

Table S4 Physicochemical properties of groundwater

	Groundwater
pH	7.882
DO (mg/L)	3.07
E_h (mV)	259.2
Mg^{2+} (mg/L)	8.34
Ca^{2+} (mg/L)	59.33
Na^+ (mg/L)	17.58
K^+ (mg/L)	2.69
Cl^- (mg/L)	39.05
NO_3^- (mg/L)	5.38
SO_4^{2-} (mg/L)	9.05
F^- (mg/L)	<1